One-dimensional resistive states in quasi-two-dimensional superconductors: Experiment and theory

M. Bell, A. Sergeev, V. Mitin, J. Bird, and A. Verevkin*
Electrical Engineering Department, University at Buffalo, Buffalo, New York 14260, USA

G. Gol'tsman
Physics Department, Moscow Pedagogical State University, 119992 Moscow, Russia
(Received 1 August 2007; published 27 September 2007)

We investigate competition between one- and two-dimensional topological excitations—phase slips and vortices—in the formation of resistive states in quasi-two-dimensional superconductors in a wide temperature range below the mean-field transition temperature T_{C0}. The widths $w=100$ nm of our ultrathin NbN samples are substantially larger than the Ginzburg-Landau coherence length $\xi=4$ nm, and the fluctuation resistivity above T_{C0} has a two-dimensional character. However, our data show that the resistivity below T_{C0} is produced by one-dimensional excitations—thermally activated phase slip strips (PSSs) overlapping the sample cross section. We also determine the scaling phase diagram, which shows that even in wider samples the PSS contribution dominates over vortices in a substantial region of current and/or temperature variations. Measuring the resistivity within 7 orders of magnitude, we find that the quantum phase slips can only be essential below this level.

DOI: 10.1103/PhysRevB.76.094521 PACS number(s): 74.81.Bd, 74.40.+k, 74.78.Na

The nature of the resistive state in superconductors attracts much attention from the physics community, since it involves fundamental phenomena and advanced concepts[1,2] such as the mechanisms of high-T_c superconductivity,[3] thermal fluctuations,[4,5] macroscopic quantum tunneling,[6–8] coherence,[9] topological excitations,[10] and phase disordering.[11] Resistive states are used in a number of quantum nanodevices, such as logic elements,[12] ultrasensitive detectors of radiation, single-photon counters, and nanocalorimeters.[13,14] Understanding resistive states in nanoscale superconductors is critical for the advancement of fundamental science and the development of novel applications.

Phase slips and vortices are elementary topological excitations which create resistive states.[1,2,10] Wires with radius less than the coherence length ξ or stripes with $w<\xi$ are one-dimensional (1D) superconductors. In 1D structures, the resistive state is produced by phase slips and is well described by the Langer-Ambegaokar-McCumber-Halperin (LAMH) theory of thermally activated phase slips (TAPSs).[1,2,4,5] At low enough temperatures, the quantum phase slips (QPSs) should be important,[6] but the magnitude of this effect and the characteristic resistance at the transition from TAPSs to QPSs are still under debate.[7,8]

In two-dimensional (2D) superconductors, the resistive state is formed by moving vortices. Above the Berezinskii-Kosterlitz-Thouless (BKT) transition temperature T_C, there is a nonzero concentration of free vortices due to thermal unbinding of vortex-antivortex pairs (VAPs).[15,16] Below T_C in an infinite 2D superconductor, VAPs are tightly bound and only a significant bias current can unbind the pairs, resulting in a nonlinear flux flow resistance. In finite size samples, free vortices can exist below T_C and produce a linear resistance at low bias currents.[15] It is commonly believed that the transition from 1D phase slip excitations to 2D vortex physics takes place at $w/\xi\sim 1$.[1,2,7,12,17] However, despite thorough studies of phase slip and vortex mechanisms, an investigation of their competition in quasi-two-dimensional superconductors is long overdue.

In this paper, we study the resistive transition in NbN superconducting samples of thickness $d=4$ nm, width $w=100$ nm, and a relatively short coherence length, $\xi\simeq 4$ nm, primarily due to the short electron mean free path. Thus, our samples are quasi-2D superconductors with a ratio $w/\xi=25$. We show that in these samples, 1D phase slip strips (PSSs) are responsible for resistive state formation in a wide temperature range, extending far below the BKT transition. We also determine the phase diagram and show its scaling character.

Our structures were fabricated from NbN superconducting films, which were deposited on *R*-plane sapphire substrates by dc reactive magnetron sputtering. Details of the film deposition process are described in Ref. 18. The samples were then patterned using direct electron beam lithography and reactive ion etching. Parameters for each of the samples are shown in Table I.

Transport measurements were performed in vacuum. Four-point resistance measurements with rf-filtered leads were made with a lock-in amplifier for bias currents ranging from 10 to 300 nA. A four-point dc measurement setup with rf-filtered leads was used for higher currents ranging from 500 nA to 1 μA. In Fig. 1, we present the resistance vs temperature obtained for both samples S1 [Fig. 1(a)] and S2 [Fig. 1(b)] at a bias current of 10 nA.

We begin by investigating the resistivity fluctuation region right above the mean-field superconducting transition T_{C0}. The insets in Figs. 1(a) and 1(b) show the resistivity on a linear scale, just above the superconducting transition for both samples. Our analysis shows that the data obtained are well described by the Aslamazov-Larkin (AL) fluctuation conductivity,[19]

TABLE I. Sample parameters: the sample thickness (d), length (L), and width (w); the mean-field transition temperature (T_{C0}); the normal resistivity (ρ_N); and the Ginzburg-Landau coherence length (ξ). T_{C0} and ρ_N were determined from the AL conductivity above T_{C0}; ξ is found from the LAMH fit below T_{C0}.

Sample	d (nm)	L (μm)	w (nm)	T_{C0} (K)	ρ_N ($\mu\Omega$ cm)	ξ (nm)
S1	4±0.2	500	100±5	11.6	264	4.0
S2	4±0.2	30	100±5	11.9	252	4.0

$$\sigma_{AL} = \frac{e^2}{16\hbar d}\frac{T_{C0}}{T - T_{C0}}. \tag{1}$$

Fitting the change in resistivity by $\delta\rho(T) = -\sigma_{AL}\rho_N^2$, we aim to determine T_{C0} and ρ_N. The obtained parameters are presented in Table I. Note that we do not study the corrections very close to T_{C0} and limit the range of data fitted to relatively small corrections, $\delta\rho/\rho_N \leqslant 0.1$. Our fits in the insets of Fig. 1 show that in this temperature range, the AL term in the form of Eq. (1) dominates over other possible contributions.

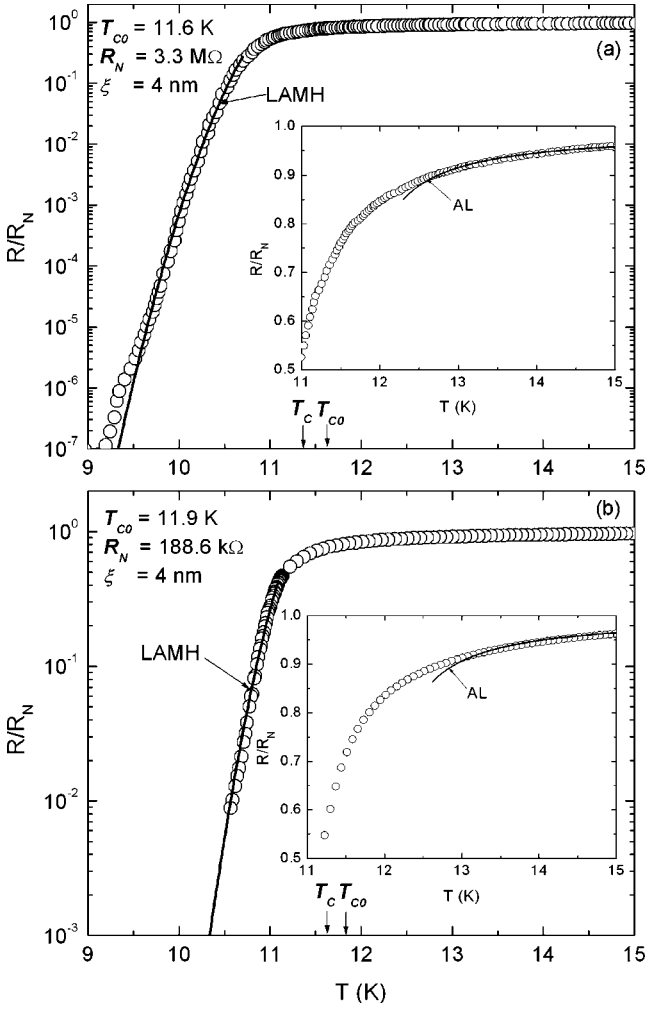

FIG. 1. Normalized resistance R/R_N vs T for the samples (a) S1 and (a) S2; the solid lines represent fits by the LAMH theory. Insets show the resistance above T_{C0}, and solid lines are the AL fits.

Next, we investigate the resistivity below T_{C0} in the framework of the LAMH theory for TAPSs. The LAMH expression for resistance at low bias currents is[1,4,5]

$$R_{LAMH}(T) = \frac{4R_0 L}{\pi\xi(T)}\frac{T_{C0} - T}{T_{C0}}\sqrt{\frac{\Delta F}{k_B T}}\exp\left(-\frac{\Delta F}{k_B T}\right), \tag{2}$$

$$\Delta F(T) \approx 0.4k_B(T_{C0} - T)\frac{w}{\xi(T)}\frac{R_0}{R_{sq}}, \tag{3}$$

where $R_0 = h/2e^2 \simeq 13$ kΩ is the resistance quantum, $\xi(T) = \xi(1 - T/T_C)^{-1/2}$ is the temperature dependent coherence length, and $R_{sq} = \rho_N/d$ is the normal state resistance per square.

In Fig. 1, we show fits of our $R(T)$ data to LAMH formulas [Eqs. (2) and (3)], which are in excellent agreement for both samples. In this fitting procedure, we used only one fitting parameter ξ, which was found to be 4.0 nm for both samples. This value is in good agreement with $\xi \approx 0.6\sqrt{\hbar D/k_B T_{C0}} = 3.4$ nm, determined with the diffusion coefficient $D \simeq 0.5$ cm^2/s, which can be obtained from the resistivity of our films.[20]

Measuring the linear resistance as a function of temperature in a range of 7 orders of magnitude, we do not observe any deviation from LAMH theory, which is usually considered as a manifestation of QPSs. Although several groups reported observations of QPSs,[6–8] the data and its interpretation remain controversial. While various phenomenological and microscopic models of QPS formation have been proposed, experimentalists appeal to the phenomenological theory suggested by Giordano.[6] In this approach, the QPS contribution to the resistivity can be described by Eq. (2), where $k_B T$ is replaced by $(8ak_B/\pi)(T_{C0} - T)$, with a a constant of the order of unity. Also, in this phenomenology, an additional fitting parameter b was added into $\Delta F(T)$. According to Giordano, a is a universal constant, so the crossover from TAPS to QPSs should occur at a characteristic value of $t_{cr} = T/T_{C0}$ independent of the sample cross section and material parameters. The factor b is weakly dependent on material properties and, therefore, the crossover should be observed at approximately the same value of $r_{cr} = R(t_{cr})/R_N$. In fact, the crossover was observed in In wires at $r_{cr} \simeq 10^{-2} - 10^{-3}$,[6] then in Sn wires at $r_{cr} \simeq 10^{-3} - 10^{-4}$,[7] and recently, in Al wires at $r_{cr} \simeq 10^{-4} - 10^{-5}$.[8] All data show a strong dependence of r_{cr} on the wire diameter. Other recent measurements in MoGe wires do not show any trace of QPS for

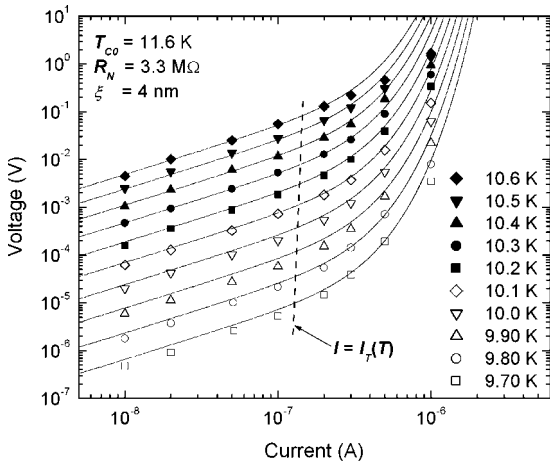

FIG. 2. Current-voltage characteristics of sample S1 at $T=9.7-10.6$ K. The solid lines are fits by the LAMH theory [Eq. (4)]. The dashed line shows the characteristic current I_T.

R/R_N spanning 11 orders of magnitude.[20] Our data support the results of Ref. 20 and show that QPSs could be important at lower temperatures and r_{cr} values.

We have also investigated nonlinear effects at bias currents ranging from 10 nA to 1 μA. The current-voltage characteristics obtained at various temperatures are shown in Fig. 2. The solid lines represent the LAMH expression,[1]

$$V(I,T) = 0.5 I_T R_{LAMH}(T) \exp(I/I_T), \tag{4}$$

where $I_T = 4ek_BT/h \simeq 0.013\ \mu\text{A/K}T$. To plot $V(I,T)$, we used the resistance R_{LAMH} [Eq. (2)] investigated previously at low currents. The dashed line in Fig. 2 represents the characteristic current I_T. As shown in Fig. 2, the results of our measurements agree with the LAMH theory for currents up to $\sim 1\ \mu$A. Deviations at higher currents are most likely due to electron heating, which will be evaluated later. Note that in thin-film quasi-2D superconductors, the heating can be localized into resistive domains, which are formed by the dissipative motion of vortices;[9] however, our data do not show such effects of local heating.

We have shown above that our data on resistivity measured in Ohmic and non-Ohmic regimes are in excellent agreement with the LAMH theory, which has been developed for quasi-1D superconductors. Why does the LAMH theory turn out to be applicable to quasi-2D samples? Generally speaking, in superconductors with width wider than ξ, the order parameter can change along the width and, therefore, resistive domains of various geometries are possible. Equations (2) and (3) take into account only simple domains in the form of PSSs, i.e., strips with width equal to ξ and a length equal to w [Fig. 3(a)]. Obviously, among other possible forms, the PSS has a minimal volume (see Fig. 3) and its generation requires a minimal energy, $\Delta F \simeq (H_c^2/8\pi)\xi w d$, where H_c is the critical magnetic field. Because of the exponential dependence of R_{LAMH} on ΔF, one can neglect domains other than PSSs.

Overall, analysis of our data in the framework of the LAMH theory strongly suggests that the resistive state in our quasi-2D NbN samples is a result of 1D PSS excitations. This observation is very interesting, because in such samples vortices are expected to dominate the resistive state. In what follows, we support the statement above by modeling the competition between 1D PSS excitations and vortices in quasi-2D superconductors.

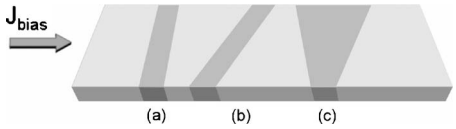

FIG. 3. Among other possible forms of resistive domains in quasi-2D superconductors, the PSS stripe (a) with width equal to ξ and a length equal to w has a minimal volume.

The vortex state critically depends on temperature with respect to the BKT transition temperature T_C, introduced for an infinitely wide film. Above T_C, there is a finite concentration of free vortices due to thermal fluctuations, while below T_C, all vortices are tightly bound into pairs. For disordered superconducting films, T_C is given by $T_C/T_{C0} = (1 + 0.54R_{sq}/R_0)^{-1}$.[21] We estimate $T_C = 11.3$ K for sample S1 and $T_C = 11.6$ K for sample S2. Since the obtained values of T_C are very close to T_{C0}, and the temperature interval $T_{C0} - T_C$ is quite narrow compared to the entire resistive transition broadening in our samples, we limit our calculations to temperatures below T_C. In this temperature range, current-induced unbinding of VAPs can occur when the Lorentz force proportional to the bias current density exceeds the force of mutual attraction between the vortex and antivortex. The threshold current which unbinds the vortex and antivortex independent of film width is given by[22]

$$I_{th} \simeq 2\kappa(T) I_T, \quad \kappa(T) = \frac{T_C - T}{T_{C0} - T_C}. \tag{5}$$

For $I \geqslant I_{th}$, the nonlinear resistance due to current-induced unbinding of vortex-antivortex pairs can be approximated by

$$R_{VAP}^{nl} \simeq 4R_N[\kappa(T) - 1](I/I_0)^{2\kappa(T)}, \tag{6}$$

where $I_0 = [w/\xi(T)]I_T$ is a characteristic current proportional to the structure width.

For $I \leqslant I_{th}$, the bias current is not sufficient to unbind VAPs, but a nonzero concentration of free vortices can still exist due to the finite size of the film.[16] These free vortices produce a linear resistance,

$$R_{VAP}^{l} \simeq 4R_N[\kappa(T) - 1]\left[\frac{\xi(T)}{w}\right]^{2\kappa(T)}. \tag{7}$$

To investigate PSS and vortex contributions to the resistance, we use Eqs. (2), (4), (6), and (7). Taking into account that the normal resistance may be represented as $R_N = R_{sq}(L/\xi)(\xi/w)$, we see that the relative contributions of PSS and vortices depend on four dimensionless parameters: I/I_T, $(T_C - T)/(T_{C0} - T_C)$, w/ξ, and R_{sq}/R_0. In Fig. 4, we present a phase diagram of the resistive states in I/I_T and $(T_C - T)/(T_{C0} - T_C)$ coordinates for samples with $w/\xi = 25$ [Fig. 4(a)] and $w/\xi = 75$ [Fig. 4(b)]. The value of R_{sq}/R_0 was

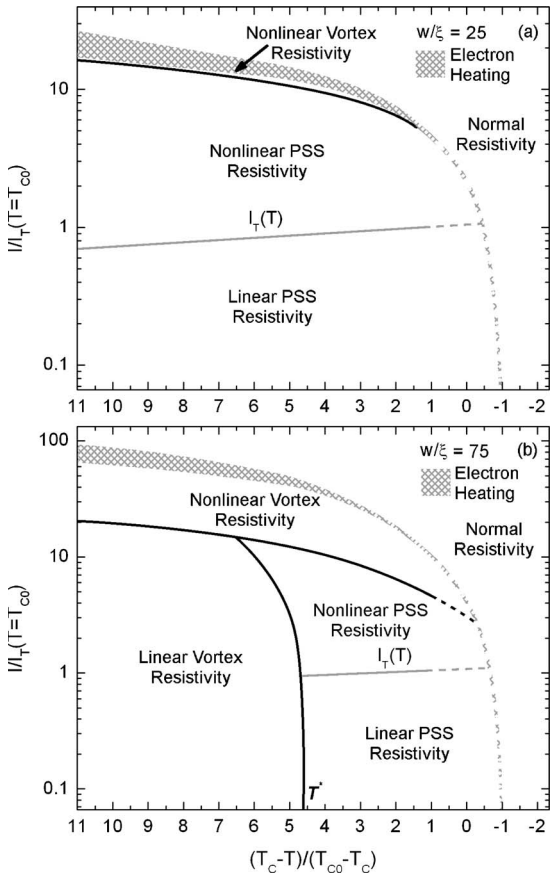

FIG. 4. The phase diagrams for samples with w/ξ of 25 and 75. The hatched pattern represents the area of significant electron heating.

taken to be 0.05, which corresponds to our NbN samples. The solid lines in Fig. 4 represent the boundary between PSS and vortex mechanisms, described by Eqs. (2) and (4), and Eqs. (6) and (7), respectively. The solid gray lines represent I_T, which separates the linear and nonlinear mechanisms related to PSSs. The nonlinear vortex mechanism dominates over others at currents which exceed the threshold current given by Eq. (5). The hatched area represents a region of strong electron heating, where the change in electron temperature $\delta\theta \simeq j^2\rho\tau_{e\text{-}ph}/C_e$ rises to (T_C-T). In these evaluations, we have used values for the electron heat capacity C_e and the electron-phonon relaxation time $\tau_{e\text{-}ph}$ from Ref. 23. Finally, the dashed segments of the boundaries in both phase diagrams represent a narrow region very close enough to T_{C0}, where the interaction between phase slips and nonequilibrium phenomena become important and, therefore, the LAMH theory is not applicable.[1]

As the sample width increases, the relative contribution of PSSs to the resistivity decreases. The phase diagram for samples with $w/\xi=75$ in Fig. 4(b) shows that, at currents below I_{th}, the PSS mechanism competes with free vortices generated below T_C due to finite size effects. While the contributions from both mechanisms decrease with increasing sample width, the PSS formation is more sensitive to the parameter w/ξ because of an exponential dependence of the PSS resistance [Eq. (2)] on $\Delta F(T)$, which, in turn, is proportional to w/ξ. Figure 5 shows that the characteristic crossover temperature T^* separating the linear PSS and vortex mechanisms strongly depends on the sample width and changes very weakly with R_{sq}. Therefore, the obtained diagram has a scaling character in the dimensionless coordinates used.

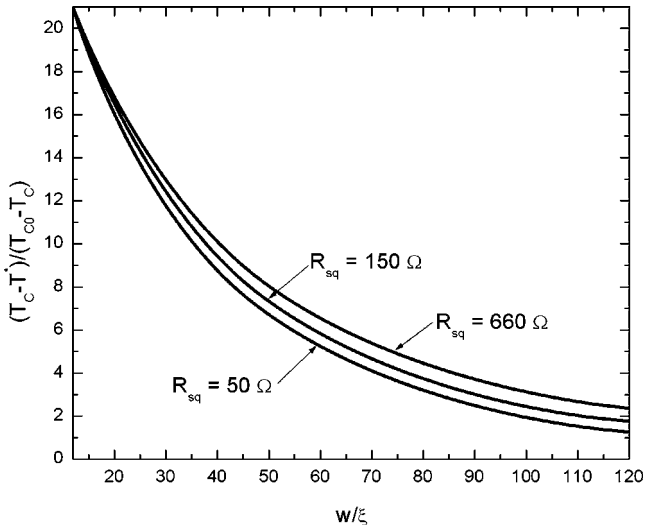

FIG. 5. The crossover temperature T^* as a function of sample width for samples with different sheet resistances.

Reviewing other experiments with NbN, let us note that the complex investigations of resistivity in 1 μm films,[24] demonstrate only effects of vortices. This result is in agreement with our modeling, which also does not show any measurable contribution of PSSs in the samples with $w/\xi=250$. In Ref. 25, samples with geometry similar to our device S2 and $T_{C0}=4.8$ K have been investigated at rather high currents, ~ 1 μA. The data of Ref. 25 have been found to be well described by the vortex-induced resistivity. This observation is also in qualitative agreement with our phase diagram, while essential effects of electron heating may also be expected. According to our modeling, samples with w/ξ in the range of 50–100 (0.2–0.4 μm for NbN) would be preferable for further experimental investigations of the boundaries between 1D and 2D excitations.

In conclusion, we have investigated the competition between the PSS and vortex excitations in the formation of resistive states in quasi-2D superconductors. Our data are in excellent agreement with the LAMH theory of TAPSs and do not show any evidence of QPS contribution. The data and modeling show that the 1D PSS mechanism dominates over the substantial range of parameters (see Fig. 4). Essentially, the creation of a PSS overlapping the sample cross section requires a significantly higher energy than the creation of a vortex or VAP. However, the PSS mechanism turns out to be more effective in producing resistance. In clean superconductors with large values of ξ, the PSS excitations will prevail over vortices in wide samples, because the phase diagram depends only on the parameter w/ξ.

The work was supported by NYSTAR. M.B. also acknowledges support from the NSF IGERT program.

*verevkin@buffalo.edu

[1] M. Tinkham, *Introduction to Superconductivity*, 2nd ed. (McGraw-Hill, New York, 1996).
[2] A. Larkin and A. Varlamov, *Theory of Fluctuations in Superconductors* (Oxford University Press, New York, 2005).
[3] P. A. Lee, N. Nagaosa, and X. G. Wen, Rev. Mod. Phys. **78**, 17 (2006).
[4] J. S. Langer and V. Ambegaokar, Phys. Rev. **164**, 498 (1967).
[5] D. E. McCumber and B. I. Halperin, Phys. Rev. B **1**, 1054 (1970).
[6] N. Giordano, Phys. Rev. Lett. **61**, 2137 (1988).
[7] M. Tian, J. Wang, J. S. Kurtz, Y. Liu, M. H. W. Chan, T. S. Mayer, and T. E. Mallouk, Phys. Rev. B **71**, 104521 (2005).
[8] F. Altomare, A. M. Chang, M. R. Melloch, Y. Hong, and C. W. Tu, Phys. Rev. Lett. **97**, 017001 (2006).
[9] A. G. Sivakov, A. M. Glukhov, A. N. Omelyanchouk, Y. Koval, P. Muller, and A. V. Ustinov, Phys. Rev. Lett. **91**, 267001 (2003).
[10] V. Pokrovsky, A. Belavin, A. Zamolodchikov, and Y. Ishimoto, arXiv:hep-th/0510214 (unpublished).
[11] S. Khlebnikov and L. P. Pryadko, Phys. Rev. Lett. **95**, 107007 (2005).
[12] J. E. Mooij and Yu. V. Nazarov, Nat. Phys. **2**, 169 (2006).
[13] A. Verevkin, J. Zhang, R. Sobolewski, A. Lipatov, O. Okunev, G. Chulkova, A. Korneev, K. Smirnov, G. N. Goltsman, and A. Semenov, Appl. Phys. Lett. **80**, 4687 (2002).
[14] B. Karasik and A. Sergeev, IEEE Trans. Appl. Supercond. **15**, 618 (2005).
[15] J. M. Kosterlitz and D. J. Thouless, J. Phys. C **6**, 1181 (1973).
[16] B. I. Halperin and D. R. Nelson, J. Low Temp. Phys. **36**, 599 (1979).
[17] D. Pekker, A. Bezryadin, D. S. Hopkins, and P. M. Goldbart, Phys. Rev. B **72**, 104517 (2005).
[18] G. N. Gol'tsman, K. Smirnov, P. Kouminov, B. Voronov, N. Kaurova, V. Drakinsky, J. Zhang, A. Verevkin, and R. Sobolemski, IEEE Trans. Appl. Supercond. **13**, 192 (2003).
[19] L. G. Aslamazov and A. I. Larkin, Phys. Lett. **26A**, 238 (1968).
[20] A. A. Rogachev, A. T. Bollinger, and A. Bezryadin, Phys. Rev. Lett. **94**, 017004 (2005).
[21] M. R. Beasley, J. E. Mooij, and T. P. Orlando, Phys. Rev. Lett. **42**, 1165 (1979).
[22] A. T. Fiory, A. F. Hebard, and W. I. Glaberson, Phys. Rev. B **28**, 5075 (1983).
[23] Y. P. Gousev, A. D. Semenov, G. N. Goltsman, A. V. Sergeev, and E. M. Gershenzon, Physica B **194**, 1355 (1994).
[24] R. Barends, M. Hajenius, J. R. Gao, and T. M. and Klapwijk, Appl. Phys. Lett. **87**, 263506 (2005).
[25] A. Engel, A. D. Semenov, H.-W. Hbers, K. Il'in, and M. Siegel, Physica C **444**, 12 (2006).